WELCOME FROM THE CONFERENCE CHAIRS

R. Cengiz Ertekin
Conference Co-Chair
OMAE 2009

H. Ronald Riggs
Conference Co-Chair
OMAE 2009

Aloha!

On behalf of the OMAE 2009 Organizing Committee, it is a pleasure to welcome you to Honolulu, Hawaii for OMAE 2009, the **28th International Conference on Ocean, Offshore and Arctic Engineering**. This is the first conference with the new name, which reflects the expanded focus of the OOAE Division and the conference.

OMAE 2009 is dedicated to the memory of Prof. Subrata Chakrabarti, an internationally known offshore engineer, who passed away suddenly in January. Subrata was the Offshore Technology Symposium coordinator, and he was also the Technical Program Chair for OMAE 2009. He was involved in the development of the OMAE series of conferences from the beginning, and his absence will be sorely felt.

OMAE 2009 has set a new record for the number of submitted papers (725), despite an extremely challenging economic environment. The conference showcases the exciting and challenging developments occurring in the industry. Program highlights include a special symposium honoring the important accomplishments of Professor Chiang C. Mei in the fields of wave mechanics and hydrodynamics and a joint forum of 'Offshore Technology', 'Structures, Safety and Reliability' and 'Ocean Engineering' Symposia on Shallow Water Waves and Hydrodynamics. We believe the OMAE 2009 program will be one of the best ever. Coupled with our normal Symposia, we will also have special symposia on:

- Ocean Renewable Energy
- Offshore Measurement and Data Interpretation
- Offshore Geotechnics
- Petroleum Technology

We want to acknowledge and thank our distinguished keynote speakers: Robert Ryan, Vice President – Global Exploration for Chevron; Hawaii Rep. Cynthia Thielen, an environmental attorney who has a special passion for ocean renewable energy; and John Murray, Director of Technology Development with FloaTEC, LLC.

A conference such as this cannot happen without a group of dedicated individuals giving their time and talents to the conference. In addition to the regular symposia coordinators, the coordinators of the special symposia deserve many thanks for their efforts to organize new areas for OMAE. We also want to express our appreciation to Dan Valentine, who stepped into the Technical Program Chair position

on very short notice, following Subrata's passing. We also want to thank Ian Holliday and Carolina Lopez of Sea to Sky Meeting Management, who have done a great job with the organization. Thanks also go to Angeline Mendez from ASME for the tremendous job she has done handling the on-line paper submission and review process.

Honolulu is one of the top destinations in the world. We hope that you and your family will be able to spend some time pre or post conference enjoying the island of Oahu. Whether you're learning to surf in legendary Waikiki, hiking through the rich rainforests of Waimea Valley, or watching the brilliant pastels of dusk fade off of Sunset Beach, you'll find variety at every turn on Oahu.

Mahalo nui loa,

R. Cengiz Ertekin and H. Ronald Riggs, University of Hawaii
OMAE 2009 Conference Co-Chairmen

MESSAGE FROM THE TECHNICAL PROGRAM CHAIR

Daniel T. Valentine
Technical Program Chair
OMAE 2009

Welcome to the **28th International Conference on Ocean, Offshore and Arctic Engineering** (OMAE 2009). This is the 28th conference in the OMAE series guided by and influenced significantly by our friend and colleague, Subrata K. Chakrabarti. It was a shock for me to learn that he had passed away so suddenly; all involved with this conference express sincere condolence to his family, friends and colleagues (the sentiments echoed by all of us are eloquently expressed in the dedication included in this program). It is a great honor for me to have been asked to continue his work on this conference. I and our community will miss his leadership and friendship greatly. Although this series of conferences was formally organized by ASME and the OOAE Division of the International Petroleum Technology Institute (IPTI), it was Subrata's skill and dedication to this division of ASME that made this series of conferences the success that it has been and is today.

The papers published in this CD were presented at OMAE2009 in thirteen symposia. They are:

- SYMP-1: Offshore Technology
- SYMP-2: Structures, Safety and Reliability
- SYMP-3: Materials Technology
- SYMP-4: Pipeline and Riser Technology
- SYMP-5: Ocean Space Utilization
- SYMP-6: Ocean Engineering
- SYMP-7: Polar and Arctic Sciences and Technology
- SYMP-8: CFD and VIV
- SYMP-9: C.C. Mei Symposium on Wave Mechanics and Hydrodynamics
- SYMP-10: Ocean Renewable Energy
- SYMP-11: Offshore Measurement and Data Interpretation
- SYMP-12: Offshore Geotechnics
- SYMP-13: Petroleum Technology

The first eight symposia are the traditional symposia organized by the eight technical committees of the OOAE Division. The other symposia are specialty symposia organized and encouraged by members of the technical committees to focus on topics of current interest. The 9th symposium was organized to recognize the contributions of Professor C. C. Mei. Symposia 10, 11, 12 and 13 offer papers in the areas of renewable energy, measurements and data interpretation, geotechnical and petroleum technologies as they relate to ocean, offshore and polar operations of industry, government and academia.

The first symposium, Symposium 1: Offshore Technology was always Subrata Chakrabarti's project. It was typically the largest of the symposia at OMAE. His exemplary work on this symposium provided the experience and guidance for others to continue to develop the other symposia. Symposium 1 in conjunction with the OMAE series of conferences is Subrata's legacy. The Executive Committee has a most difficult yet honorable task of finding a successor to carry on this important annual symposium in offshore engineering. We are all grateful

for the inspiration and encouragement provided to all of us by Subrata.

Please enjoy the papers and presentations of OMAE2009.

Daniel T. Valentine, Clarkson University, Potsdam, New York
OMAE2009 Technical Program Chair

INTERNATIONAL ADVISORY COMMITTEE

- R.V. Ahilan, Noble Denton, UK
- R. Basu, ABS Americas, USA
- R. (Bob) F. Beck, University of Michigan, USA
- Pierre Besse, Bureau Veritas, France
- Richard J. Brown, Consultant, Houston, USA
- Gang Chen, Shanghai Jiao Tong University, China
- Jen-hwa Chen, Chevron Energy Technology Company, USA
- Yoo Sang Choo, National University of Singapore, Singapore
- Weicheng C. Cui, CSSRC, Wuxi, China
- Jan Inge Dalane, Statoil, Norway
- R.G. Dean, University of Florida, USA
- Mario Dogliani, Registro Italiano Navale, Italy
- R. Eatock-Taylor, Oxford University, UK
- George Z. Forristall, Shell Global Solutions, USA
- Peter K. Gorf, BP, UK
- Boo Cheong (B.C.) Khoo, National University of Singapore, Singapore
- Yoshiaki Kodama, National Maritime Research Institute, Japan
- Chun Fai (Collin) Leung, National University of Singapore, Singapore
- Sehyuk Lee, Samsung Heavy Industries, Japan
- Eike Lehmann, TU Hamburg-Harburg, Germany
- Henrik O. Madsen, Det Norske Veritas, Norway
- Adi Maimun Technology University of Malaysia, Malaysia
- T. Miyazaki, Japan Marine Sci. & Tech Centre, Japan
- T. Moan, Norwegian University of Science and Technology, Norway
- G. Moe, Norwegian University of Science and Technology, Norway
- A.D. Papanikolaou, National Technical University of Athens, Greece
- Hans Georg Payer, Germanischer Lloyd, Germany
- Preben T. Pedersen, Technical University of Demark, Denmark
- George Rodenbusch, Shell Intl, USA
- Joachim Schwarz, JS Consulting, Germany
- Dennis Seidlitz, ConocoPhillips, USA
- Kirsi Tikka, ABS Americas, USA
- Chien Ming (CM) Wang, National University of Singapore, Singapore
- Jaap-Harm Westhuis, Gusto/SBM Offshore, Netherlands
- Ronald W. Yeung, University of California at Berkeley, USA

COPYRIGHT INFORMATION

Proceedings of the
ASME 2009 28th International Conference on Ocean, Offshore and Arctic Engineering (OMAE2009)
May 31 - June 5, 2009 • Honolulu, Hawaii, USA

ISBN 978-0-7918-3844-0
Order No. I811DV

Proceedings of the ASME 2009 28th International Conference on Ocean, Offshore and Arctic Engineering
OMAE2009
May 31 - June 5, 2009, Honolulu, Hawaii, USA

OMAE2009-79366

REAL TIME ESTIMATION OF SHIP MOTIONS IN SHORT CRESTED SEAS

P. Naaijen
Delft University of Technology
Delft, The Netherlands

R.R.T. van Dijk
MARIN
Wageningen,
The Netherlands

R.H.M. Huijsmans
Delft University of Technology
Delft, The Netherlands

A.A. El-Mouhandiz
MARIN
Wageningen
The Netherlands

ABSTRACT

The presented research is part of the development of an onboard wave and motion estimation system that aims to predict wave elevation and vessel motions some 60 - 120 s ahead, using wave elevation measurements by means of X-band radar.

In order to validate the prediction model, scale experiments have been carried out in short crested waves for 3 different sea states with varying directional spreading, during which wave elevation and vessel motions were measured.

To compare predicted and measured wave elevation, three wave probes were used at different distances from a large set of wave probes that was used as input to the model . At one of the prediction locations, also tests were performed to measure vessel motions.

This setup allowed validation of a method that was used for initializing the linear wave prediction and ship motion prediction model.

Various observations and conclusions are presented concerning optimal combinations of prediction model parameters, probe set-up and sea state.

INTRODUCTION

Within an international joint industry project called OWME (Onboard Wave and Motion Estimation) a system is being developed which aims to predict ship motions some 60 seconds ahead. The main purpose of such a system is to increase safety and operability during offshore operations that are critical with regard to vessel motions, e.g. top-site installation (float-over or lifting), helicopter landing on floating vessel and LNG offloading connection. Use is being made of newest wave sensing techniques by means of X-band radar: The Ocean Waves' WAMOS II radar image processing software is capable of providing real-time time traces of wave elevation at a large number of locations.

This paper describes the validation of a model used to compute a deterministic prediction of wave elevation and ship motion by using remote wave elevation measurements in short crested waves. Linear theory is used resulting in a very simple and straightforward propagation model. The challenging part is within the initialization of this model which is the main focus of the present study.

To assess the accuracy of the prediction, extended model tests have been carried out at the Maritime Research Institute Netherlands (MARIN). During these experiments the 2 dimensional wave field was measured by using a large array of wave probes. The measured wave field is used to predict wave elevation and ship motion at various distant locations. The predictions are validated by means of measurements of both wave elevation and vessel motions at the prediction location.

EXPERIMENTS

Wave measurements

As mentioned the present study aims to predict wave elevation and vessel motion in a deterministic way using measured time traces of wave elevation at various locations. To validate the model that will be described in the next paragraph, model experiments at a scale of 1:70 were carried out at MARIN, the Netherlands.

For a selection of 3 short crested wave conditions, wave elevation was recorded by means of a wave probe array existing of 10 x 10 wire-type wave gauges.

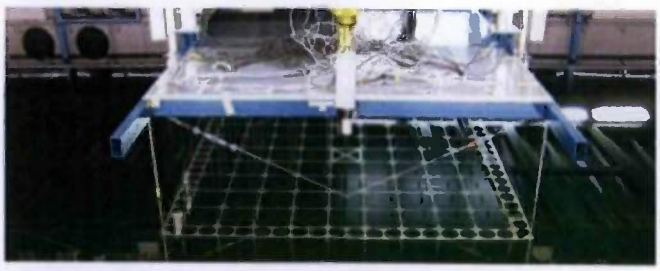

Figure 1, 10 x 10 wave gauge array

Tests were repeated with the wave gauge array positioned at different locations in the basin, thus obtaining a relatively large number of wave measurements that could be used to optimize and validate the prediction model. Figure 2 shows all wave gauge array positions for which tests were performed. Positions 1, 2 and 3 are the locations for which predictions will be made and compared with the measurements. The probes at the remaining locations are used as input for the model. The main wave direction is in positive X direction as indicated in the figure.

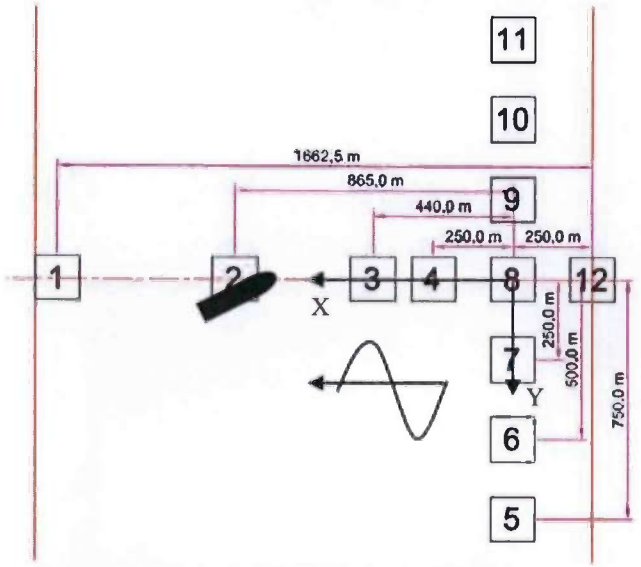

Figure 2, wave gauge array positions

As the different tests were not performed simultaneously, checks were carried out in order to confirm that different wave tests are reproducible. Figure 3 shows a sample of two wave measurements from different tests, measured at the same location. As can be seen good reproducibility is obtained.

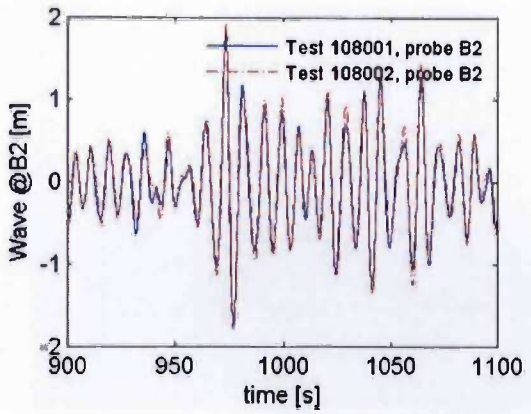

Figure 3, comparison of measured wave elevation during different tests at identical locations

Concerning the wave conditions the choice was made only to vary the amount of directional spreading. (The effect of wave steepness was examined in earlier work. (Naaijen et al. [9])).
Tests were performed for a Jonswap spectrum with a peak period T_p of 9.0 s, significant wave height H_s of 2.5 m and peakedness factor γ of 3.3.
To include directional wave spreading the following spreading function was used:

$$D(\mu) = D_0 \cdot \cos^{2s}(\mu - \mu_0)$$

with

$$D_0 = \frac{1}{\int_{\mu_0-90}^{\mu_0+90} \cos^{2s}(\mu - \mu_0)\, d\mu} \qquad (1)$$

and

$$S(\omega, \mu) = S(\omega) \cdot D(\mu)$$

Three different values for the spreading parameter s were used, being 4, 10, and 50 corresponding to very short crested wind waves, average wind waves and an average swell respectively. (Measurements at position #5, #6, #10 and #11 as indicated in Figure 2 were only performed for the tests with s=10.)
For practical reasons concerning the wave maker, the directionality was cut off leaving the sector of -15 deg – 15 deg for s=50, -30 deg – 30 deg for s=10 and -45 deg – 45 deg for s=4.

Ship motion measurements

Apart from wave elevation measurements, motions of a model of an offshore support vessel, without forward speed, located at position #2 (see Figure 2) were recorded. The model, being kept in position by a soft mooring system such that the relative wave direction was 165 degrees, is depicted in Figure 4.

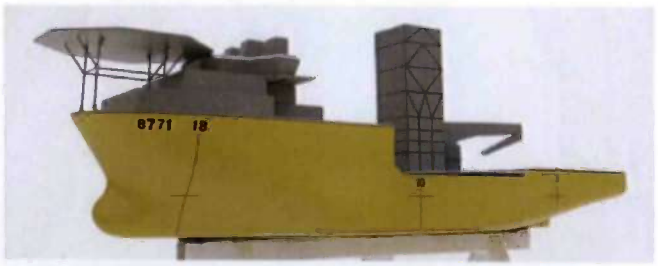

Figure 4, 1:70 model of offshore support vessel

The main particulars of the vessel are:

L_{PP}	94.2 [m]	- Length between perpendiculars
L_{WL}	101.5 [m]	- Length on waterline

B	21.0 [m]	- Breadth max.
T_F	6.0 [m]	- Draught fore
T_A	6.0 [m]	- Draught aft

Focusing on the prediction of vertical motions, mainly heave and pitch motions were considered, of which the RAO's were determined using a linear 3D diffraction program. Additional tests were carried out in irregular (white noise) long crested waves for relative wave directions varying from bow to bow quartering. Calculated RAO's appeared to be in good agreement with the RAO's determined from the mentioned experiments.

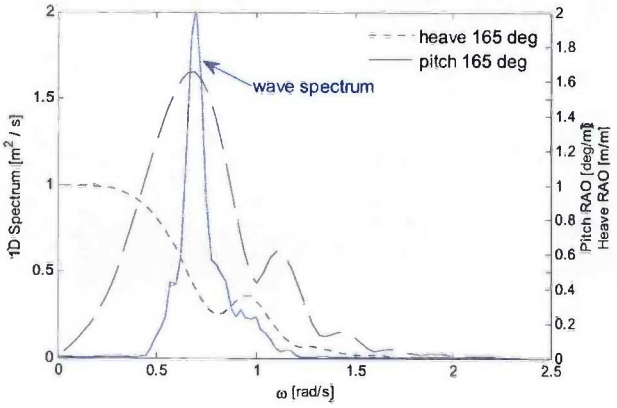

Figure 5, 1D wave spectrum and RAO's for relative wave direction of 165 deg.

Figure 5 shows the calculated heave and pitch RAO's together with the one-dimensional wave spectrum.

PROPAGATION MODEL

The theoretical model used to describe the wave field is a linear superposition of cosine waves with different frequencies traveling in different directions:

$$\zeta_j(t) = \Re\left\{\sum_{n=1}^{N/2}\sum_{m=1}^{M}\zeta_{anm}\cdot e^{i\left(\omega_n t - k_n x_j\cdot\cos(\mu_{nm}) - k_n y_j \sin(\mu_{nm}) + \varepsilon_{nm}\right)}\right\} \quad (2)$$

where:

$\Re$ = real part

ζ_{anm} = amplitude of frequency component in propagation direction μ_{nm},

ω_n = frequency of component n

k_n = wave number of component n

x_j, y_j = co-ordinates of location j

μ_{nm} = propagation direction of directional component m for frequency n

ε_{nm} = initial phase angle of component nm

M = number of directional components per frequency

From Fourier analysis, frequency components of the measured time traces at J locations can be obtained, corresponding to the following representation :

$$\tilde{\zeta}_j(t) = \Re\left\{\sum_{n=0}^{N/2}\tilde{\zeta}_{anj}e^{i\left(\omega t + \tilde{\varepsilon}_{nj}\right)}\right\} \quad (3)$$

where:

j = index of location for which time trace is provided

n = index of frequency component

N=number of samples of considered time trace

$\tilde{\zeta}_{anj}, \tilde{\varepsilon}_{nj}$ = amplitude and phase angle for frequency component n of measured time trace at location j following from FFT

From a predefined number M of directional components to be used in equation (2), the discrete wave directions μ_{nm} were chosen as was suggested by Zhang [1]: the average directional wave spectrum was determined from the measurements by means of the MLM method. For each frequency the energy content was examined and the direction of the most energetic component was identified. Ignoring on both sides of this most energetic direction a predefined small amount of wave energy, a range of wave directions is obtained that is divided into M segments whose center values are used for μ_{nm}. (The values of μ_{nm} determined this way will be frequency dependent which is why a double index nm is used.) Figure 6 shows an example of discrete ω_n - μ_{nm} combinations (marked with dots) determined as described above for M=10, together with the underlying two dimensional spectrum for the wave condition with s=10.

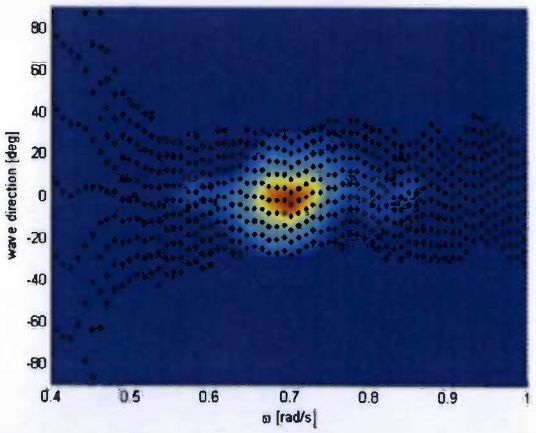

Figure 6, directional wave spectrum for s=10 and discrete components used in representation

As an estimate for the wave component amplitudes ζ_{nmi}, the spectral values $S(\omega,\mu)$ were converted to amplitudes:

$$\zeta_{nmi} = \sqrt{2S(\omega_n, \mu_m)\,d\omega d\mu} \quad (4)$$

Where:
$d\mu$ = the band width of each of the M segments mentioned above

This way the only unknowns left in equation (2) are the initial phase angles ε_{nm}.

By assuming that the above 2D representation of a wave time trace at location j (equation (2)) should equal the measured trace represented by (equation (3)), the unknown initial phase angles in (2) can be solved. This is done by considering a frequency domain representation of both measurement and 2D representation.

One method to solve the unknown phase angles is proposed by Zhang [1]:
For each frequency, an error can be defined as follows:

$$\Delta_{nj} = \tilde{\zeta}_{anj} \cdot e^{i\tilde{\varepsilon}_{nj}} - \sum_{m=1}^{M} \zeta_{anm} \cdot e^{i\left(-k_n x_j \cdot \cos(\mu_{nm}) - k_n y_j \sin(\mu_{nm}) + \varepsilon_{nm}\right)} \quad (5)$$

The unknown initial phase angles can be solved by minimizing a target function Rn defined by the sum over all J locations of the absolute squared error:

$$R_n = \sum_{j=1}^{J} \left|\Delta_{jn}\right|^2 = \sum_{j=1}^{J} \left(\Re\{\Delta_{jn}\}\right)^2 + \left(\Im\{\Delta_{jn}\}\right)^2 \quad (6)$$

Another way to solve the phase angles is by defining a matrix vector equation, Ax=b as given in equation (7), and solving this.

$$A \cdot x = b =$$

$$\begin{pmatrix} \zeta_{an1} \cdot e^{i\left(-k_n x_1 \cdot \cos(\mu_{n1}) - k_n y_1 \sin(\mu_{n1})\right)} & \cdots & \zeta_{anM} \cdot e^{i\left(-k_n x_1 \cdot \cos(\mu_{nM}) - k_n y_1 \sin(\mu_{nM})\right)} \\ \vdots & \ddots & \vdots \\ \zeta_{an1} \cdot e^{i\left(-k_n x_J \cdot \cos(\mu_{n1}) - k_n y_J \sin(\mu_{n1})\right)} & \cdots & \zeta_{anM} \cdot e^{i\left(-k_n x_J \cdot \cos(\mu_{nM}) - k_n y_J \sin(\mu_{nM})\right)} \end{pmatrix} \cdot \begin{pmatrix} e^{i\varepsilon_{n1}} \\ \vdots \\ e^{i\varepsilon_{nM}} \end{pmatrix} = \begin{pmatrix} \tilde{\zeta}_{an1} \cdot e^{i\tilde{\varepsilon}_{n1}} \\ \vdots \\ \tilde{\zeta}_{anJ} \cdot e^{i\tilde{\varepsilon}_{nJ}} \end{pmatrix} \quad (7)$$

Applying a Singular Value Decomposition (SVD) on A as done by Janssen et. al. [4] appeared to give the best results. All results and conclusions mentioned in next paragraphs are based on the latter method.
Having solved the phase angles from equation (2), the wave elevation can be calculated at any time and any location by substituting the desired values for t, x_j and y_j in the equation. However, in order to ensure physical significance of the prediction, t, x_j and y_j have to be chosen within certain limits. This will be explained in more detail in the next paragraph.
Using the RAO's for the ship motions (obtained from linear 3D diffraction calculations) a ship motion prediction can be made in a straight forward way:

$$x_{kj}(t) = \Re\left(\sum_{n=1}^{N/2}\sum_{m=1}^{M} \zeta_{anm} \cdot RAO_{knm} \cdot e^{i\left(\omega_n t - k_n x_j \cdot \cos(\mu_{nm}) - k_n y_j \sin(\mu_{nm}) + \varepsilon_{nm} + \varepsilon_{knm}\right)}\right) \quad (8)$$

where:
x_{kj} = ship motion in mode k (k = 1...6)
RAO_{knm} = frequency and direction dependent response amplitude operator for mode k
ε_{knm} = frequency and direction dependent phase angle for mode k

PREDICTABILITY

Having described the propagation model in the previous chapter, some attention is paid to the question how the difference between real surface waves and our representation of them effects the predictability of those surface waves.
Let's reconsider equation (2). If no restrictions are put to the domain in space (x_j, y_j) and time (t) for which we consider this representation to be valid, we practically assume it to be able to describe the entire ocean for an unlimited period of time.
Obviously, this isn't a realistic assumption. The validity of the representation as given in equation (2) will be limited in space and time.
To discuss these limitations, the one-dimensional case is revisited here briefly. The space-time diagram for a long crested wave traveling in positive X-direction showing the predictable zone is depicted in Figure 7.

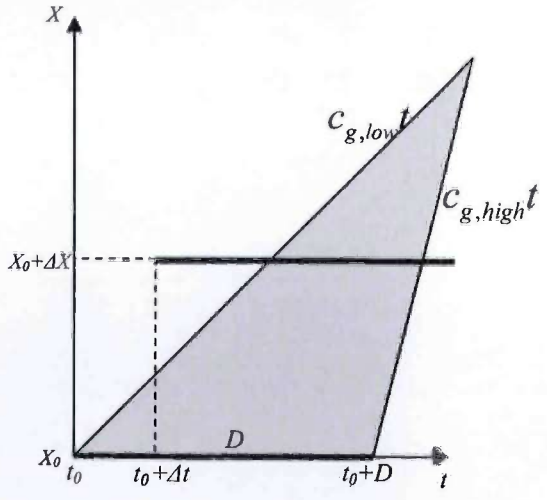

Figure 7, predictable zone long crested waves

In this diagram, introduced by Morris et al [7] and used as well by Edgar et al [8] and Naaijen et al [9], the triangles indicate the zone in space and time where the wave elevation can be predicted or reconstructed using a recorded time trace of the wave elevation which is represented by the horizontal line at the base of the triangle.
The second horizontal line represents the prediction based on this recorded time trace, ΔX away from the measurement location, shifted Δt seconds ahead. Only its part within the predictable zone (gray triangle) is supposed to be useful.
In the mentioned publications the slopes of the left and right boundaries of the predictable zone were considered to equal the phase velocity of the shortest and longest wave components present in the recorded time trace. However, as explained by Wu [10], it is not the phase velocity but the group velocity of the shortest and longest wave components that governs the size of the predictable zone. This also explains that it was observed during the experiments by Naaijen et al [9] that predictions of the wave elevation could be extended further into the future than expected based on the predictable zone bounded by the highest and lowest *phase* velocities: when applying a long enough duration D of the recorded wave elevation, only the fastest wave components will limit the prediction and as their group velocity is lower than their phase velocity, the steepness of the right-hand boundary is decreased, meaning that the prediction can be extended further into the future.

The concept of the predictable zone can be extended for the three-dimensional case. Considering the three-dimensional wave field to be a superposition of wave components traveling in different directions, a similar predictable zone diagram can be constructed for one specific traveling direction. See Figure 8.

For any point in space and time, the wave elevation due to all components traveling in the considered direction is a superposition of all frequency components traveling in that direction. Depending on which point in space and time is considered, not all these components might originate from the measurement. The highest and lowest group velocities of those components just originating from the measurement for a given prediction point in space and time (x_p, y_p, t_p) can be defined as respectively:

$$c_{g1} = \left(\left(x_p - \tilde{x}\right)\cos(\mu) + \left(y_p - \tilde{y}\right)\sin(\mu)\right)/\left(t_p - D\right)$$
$$c_{g2} = \left(\left(x_p - \tilde{x}\right)\cos(\mu) + \left(y_p - \tilde{y}\right)\sin(\mu)\right)/t_p \quad (9)$$

Where a tilde denotes the measurement location.
Denoting ω_1 and ω_2 as the corresponding wave frequencies and ω_{low} and ω_{high} as the frequencies of the shortest and longest wave components that occur in the wave field, an error estimate for the predicted wave elevation can be defined as the relative amount of wave energy represented by those components at (x_p, y_p, t_p) that do not originate from the measurement:

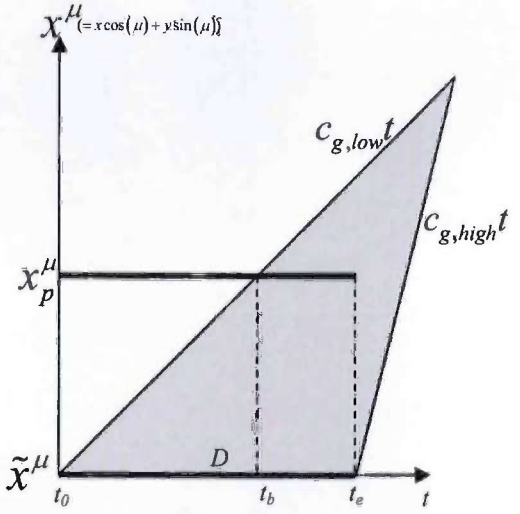

Figure 8, predictable zone for one directional component of a short crested sea

$$Err\left(x_p, y_p, t_p\right) = \left(1 - \frac{\int_0^{2\pi}\int_{\omega_1(\mu)}^{\omega_2(\mu)} S(\omega,\mu)\,d\omega d\mu}{\int_0^{2\pi}\int_{\omega_{low}}^{\omega_{high}} S(\omega,\mu)\,d\omega d\mu}\right)^{1/2} \quad (10)$$

As described in the previous chapter multiple probe records are used to find the representation of the wave field given by equation (2). However, keeping in mind the limited representing capabilities in space and time of this representation, it can only represent a decomposition of one probe record.
Imagine that for one specific direction the frequency components in the three-dimensional wave representation represent a decomposition of a measurement of length D at location $\left(\tilde{x}, \tilde{y}\right)$.

Figure 8 shows that a measurement at location $\left(x_p, y_p\right)$ can only be represented by this decomposition between t_b and t_e. (The vertical axis in Figure 8 corresponds with the spatial coordinate x^{μ}, parallel to the traveling direction of the considered wave components.)
The short wave components present in the part before t_b do not originate from the location $\left(\tilde{x}, \tilde{y}\right)$. For any point in time of the wave elevation time trace at $\left(x_p, y_p\right)$, the error Err as

defined in equation (10) can be determined. A representative mean error value for the whole time trace at (x_p, y_p) can then be defined as follows:

$$Err_{mean}(x_p, y_p) = \frac{1}{D} \int_{t_0}^{t_0+D} Err(x_p, y_p, t)dt \qquad (11)$$

So when attempts are made to find a three-dimensional wave field representation (equation(2)) that yields for a certain period of time D at location $(\tilde{x}, \tilde{y})$, only those parts of the simultaneously measured time traces at surrounding probe locations (denoted by (x_p, y_p)) should be used that are within the predictable zone. The presented methods to find the three-dimensional wave field representation are ignoring this fact since they are frequency domain methods for which it is not possible to take it into account in a straightforward way. (Wu [10] describes a time domain method for solving the three-dimensional representation for which it is possible to account for limitations in the usable part of the time traces to be used.)

In the area where the wave probes were located, Err_{mean} from equation (11) is shown for the three wave conditions for which experiments were carried out in Figure 10. Locations of the frames containing the probes whose simultaneous measurements were used for decomposing the wave field are indicated by the squares. (The dots indicate the used probe positions that appeared to give the optimal results for the considered wave condition and prediction location #2.) As can be seen the probe positions are chosen such that Err_{mean} does not exceed 0.1 for any of the conditions.

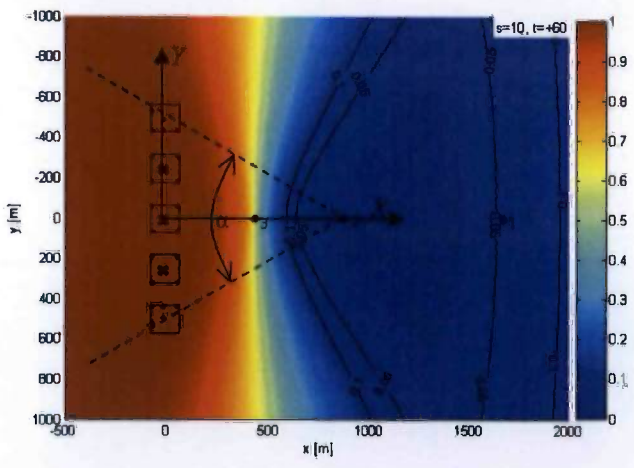

Figure 9, predictable zone for s=10 and forecast-time of 60 s

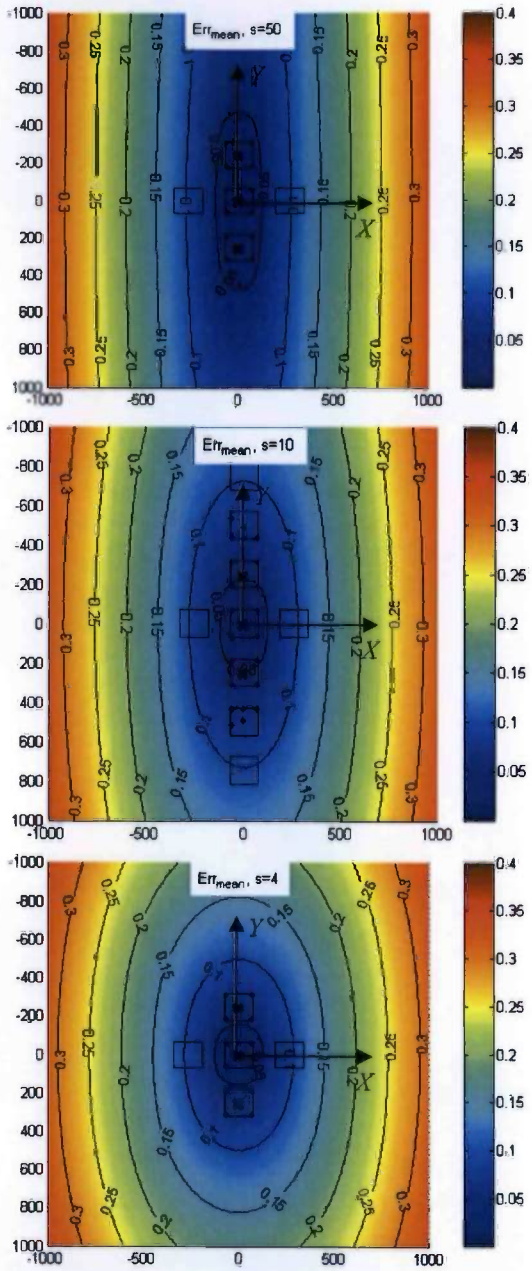

Figure 10, Err_{mean} for s=50, 10 and 4 and available probe-frame positions

When calculating the values for Err according to equation (10) for a prediction of the wave elevation at a given set of locations (x_p, y_p) for a given moment in time t_p, the optimal relative positions of measurement and prediction can be determined. For a forecast-time of 60 s and wave spreading s=10, the value of Err is presented in a similar way as was done by Blondel [11] in Figure 9.

As shown by Figure 9, prediction location #2, the location where also the ship model was located, was chosen such that it would be optimal for a 60 seconds prediction for the wave condition with s=10.

RESULTS

Several aspects have an effect on the accuracy of the wave prediction:

The setup of the probes whose measurements are used to solve the system of equation (7) should be such that their in-between distances are optimal to identify phase differences for the whole frequency range that contains wave energy. As shown by Voogt et al. [12], for one regular wave component this optimal probe distance amounts to ¼ of the wave length. Therefore it was aimed to use a probe setup that provided for all relevant frequencies in-between distances (projected in the direction of each of the wave directions used in the representation) of ¼ of the wave length.

The probe setup that appeared to give the best results for a prediction at location #2 in waves with direction spreading of s=10 is shown in Figure 9. For each of the 10 discrete wave directions that were used at the peak frequency in the two-dimensional representation, intermediate distances between the used probes, projected in each of the 10 wave directions, were determined. Figure 11 shows the 2D spectrum based on wavelength / peak wavelength ratio. The dots indicate all the available intermediate probe distances divided by ¼ peak wavelength. This way of presenting should result in a high-density of dots in the most energetic part of the spectrum for a favorable probe set-up according to the statement above.

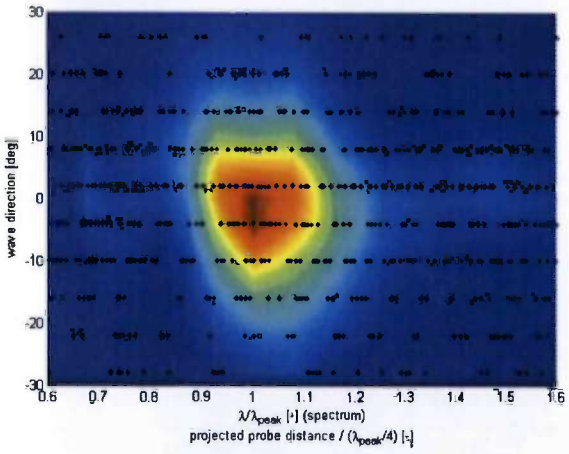

Figure 11, relative probe distances for optimal setup s=10, prediction position #2

Another important variable that effects the accuracy to a great extend is the number of directional components that is used in the representation of the wave field. With a large number of directional components, the directional spreading is better covered. However, for a given probe set-up, choosing a too large number of directional components dramatically decreases the condition of system matrix A in equation (7) resulting in poor predictions. For cases where the number of directional components was too large, it was found that adding more probe records to the equation (7) not necessarily improves the prediction. The extra probe records have to add 'information' to the system. Adding probes positioned in frame numbers 4 and 12 (Figure 2) for example did not improve the prediction for any of the cases. When the requirement to the probe set-up as stated above is fulfilled, the only way to improve the condition of the matrix is to decrease the number of wave directions. The set-ups shown in Figure 10, using 9 probes per frame as indicated by the dots, were found to give the best results for prediction at location #2. By extending the number of input measurements by using all available probes i.e. 100 per frame, no improvements were obtained.

Apart from the combination of probe set-up and number of directional components, that determines the condition of the matrix in (7), the combination of probe set-up and the prediction location was found to have a significant impact. It was observed that the use of extending the probe set-up in y-direction is limited related to the amount of wave spreading and the prediction location. See Figure 9. The angle α between the dashed lines starting from prediction location #2 equals the sector angle that bounds the directionality of the wave condition: as mentioned, for practical reasons the directionality was cut off at 30 and -30 degrees for this condition (s=10) resulting in α = 60 deg. It was observed that using measurement probes outside this angle did not improve the accuracy. This observation was found to be consistent for all combinations of prediction location and directional spreading as far as the available measurements allowed to verify it. (For the most short crested condition with s=4, measurements at positions #5, #6, #10 and #11 that would enable confirmation of this observation were not available.)

To assess the accuracy of the predictions an error value is calculated that is defined as:

$$E(t) = \frac{\sqrt{\frac{1}{N}\sum_{n=1}^{N}\left(\zeta_n(t) - \zeta_n^*(t)\right)^2}}{\sqrt{m_0^*}} \qquad (12)$$

Where:

$E(t)$ = normalized prediction error

$\zeta_n(t) = n^{th}$ realization of predicted wave elevation

$\zeta_n^*(t) = n^{th}$ realization of measured wave elevation

N = total number of realizations

$\sqrt{m_0^*}$ = RMS of measured wave elevation

Figure 12 shows the normalized error of the wave prediction averaged over N =100 realizations at location 3, 2 and 1 for the case with s=10. The vertical dashed lines indicate the

boundaries of the predictable zone in time. As expected the error increases outside the predictable zone. The solid vertical line indicates the boundary between hind cast and forecast.
Error values averaged over the predictable part of the predicted traces are given in Annex A, Table 1. All values are based on an average over 100 realizations.

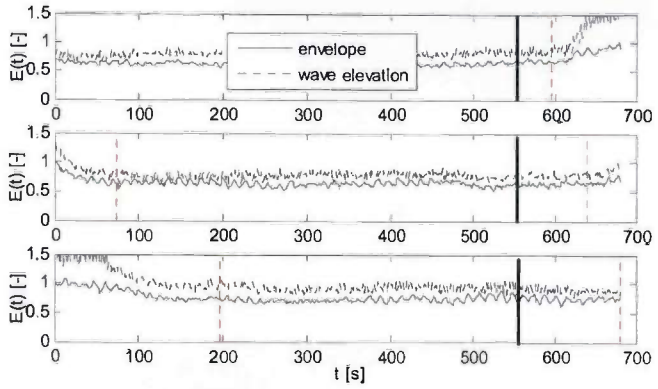

Figure 12, prediction error for locations 3,2 and 1 for s=10

Since for the applications of the onboard wave and motion estimation system we are interested in the prediction of quiet periods rather than in an exact deterministic prediction, also the envelope of the deterministic prediction has been determined: the predicted deterministic signal has been post processed by taking the absolute value of its Hilbert transform. Its error, which is defined similarly to the error of the wave elevation / ship motion itself is in general significantly smaller.
For location #2, Figure 13 shows time traces of predicted and measured wave elevation and heave and pitch motion for the case with s=10. The maximum prediction time has been determined from the measured mean two-dimensional spectrum, allowing a value of *Err* as defined in equation (10) of 0.1 and amounts to 78 s. The vertical solid line again indicates the boundary between hind cast and forecast. The rightmost vertical dashed red line indicates the end of the predictable zone in time.
In Annex B, samples of time traces are shown for all wave conditions at all prediction locations. For each prediction location the most favorable probe set-up is plotted at the right hand side of each of the corresponding time traces: The black dots indicate the used probes, the grey cross with the circle indicates the concerning prediction probe. The color indicates the *Err* value as defined in equation (10) for the allowed maximum forecast time that was aimed for (which is 30 s for probe 3, 60 s for probe 2 and 120 s for probe 1). As can be seen the chosen prediction locations match the intended forecast time well in that sense that for all conditions they are positioned in the predictable zone (where *Err* is app. 0.)

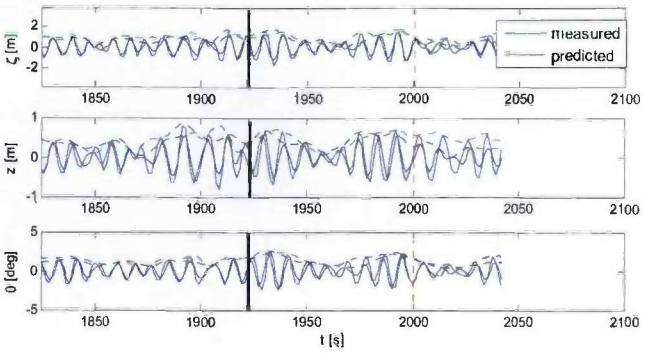

Figure 13, sample time traces of prediction and measurement of wave elevation, heave and pitch motion, location # 2, s=10

As can be seen from both the mean error values in Table 1 and from the samples of the time traces in Figure 15, predictions for s=4 are rather poor especially for locations 1 and 2. This is caused by the fact that probe measurements at locations further from the X-axes, that would be required for an optimal set-up were not available for this condition.

ACKNOWLEDGMENTS

This paper is published by courtesy of all participants and partners of the OWME-JIP for which they are gratefully acknowledged.
Special thanks to MARIN for facilitating the experiments.

REFERENCES

[1] Zhang et. al., *Deterministic wave model for short-crested ocean waves: Part I. Theory and numerical scheme*, Applied Ocean Research 21, 1999
[2] Zhang et. al., *Deterministic wave model for short-crested ocean waves: Part II. Comparison wih laboratory and field measurements*, Applied Ocean Research 21, 1999
[3] Prislin et. al., *Deterministic decomposition of deep water short-crested irregular gravity waves*, Journal of Geophysical Research, Vol. 102 No. C6, 1997
[4] Janssen et. al. *Phase resolving analysis of multidirectional wave trains*, Proceedings of the Fourth International Symposium Waves 2001, September 2-6, 2001, San Francisco, CA
[5] de Jong et. al. *A phase resolving analysis technique for short-crested wave fields*
[6] Belmont et. al. *The effect of statistically dependent phases in short-term prediction of the sea: A simulation study*, International Shipbuilding Progress Vol. 51 no.4, 2004

[7] Morris, E.L., Zienkiewicz, H.K. & Belmont M.R., 1998 *Short term forecasting of the sea surface shape*, Int. Shipbuild. Progr. 45, no.444, 383-400.

[8] Edgar D.R., Horwood J.M.K., Thurley R., Belmont M.R. *The effects of parameters on the maximum prediction time possible in short term forecasting of the sea surface shape,* International Shipbuilding Progress Vol. 47, No.451, 2000

[9] Naaijen P., Huijsmans R.H.M. 2008, *Real time wave forecasting for real time ship motion predictions,* Proc. OMAE 2008

[10] Wu, G., *Direct simulation and deterministic prediction of large-scale nonlinear ocean wave-field*, PhD Thesis, M.I.T, 2004

[11] Blondel, E., Ducrozet, G., Bonnefoy, G., Ferrant, P., *Deterministic reconstruction and prediction of non-linear wave systems,* 23rd IWWWFB, 2008, Jeju, Korea

[12] Voogt A., Bunnik T., Huijsmans R.H.M. *Validation of an analytical method to calculate wave setdown on current* Proc. OMAE 2005

ANNEX A

	s [-]	Error [-]			Error Envelope [-]			max pred [s]
prediction probe #		wave	heave	pitch	wave	heave	pitch	
1	**10**	0,915			0,703			131
2	**10**	0,778	0,802	0,748	0,639	0,597	0,547	78
3	**10**	0,744			0,607			35
	s [-]	Error [-]			Error Envelope [-]			max pred [s]
prediction probe #		wave	heave	pitch	wave	heave	pitch	
1	**4**	1,172			0,822			124
2	**4**	1,179	1,172	1,215	0,785	0,890	0,879	77
3	**4**	0,899			0,686			34
	s [-]	Error [-]			Error Envelope [-]			max pred [s]
prediction probe #		wave	heave	pitch	wave	heave	pitch	
1	**50**	0,783			0,668			138
2	**50**	0,737	0,827	0,734	0,651	0,686	0,593	83
3	**50**	0,702			0,566			37

Table 1, Averaged Error values

ANNEX B

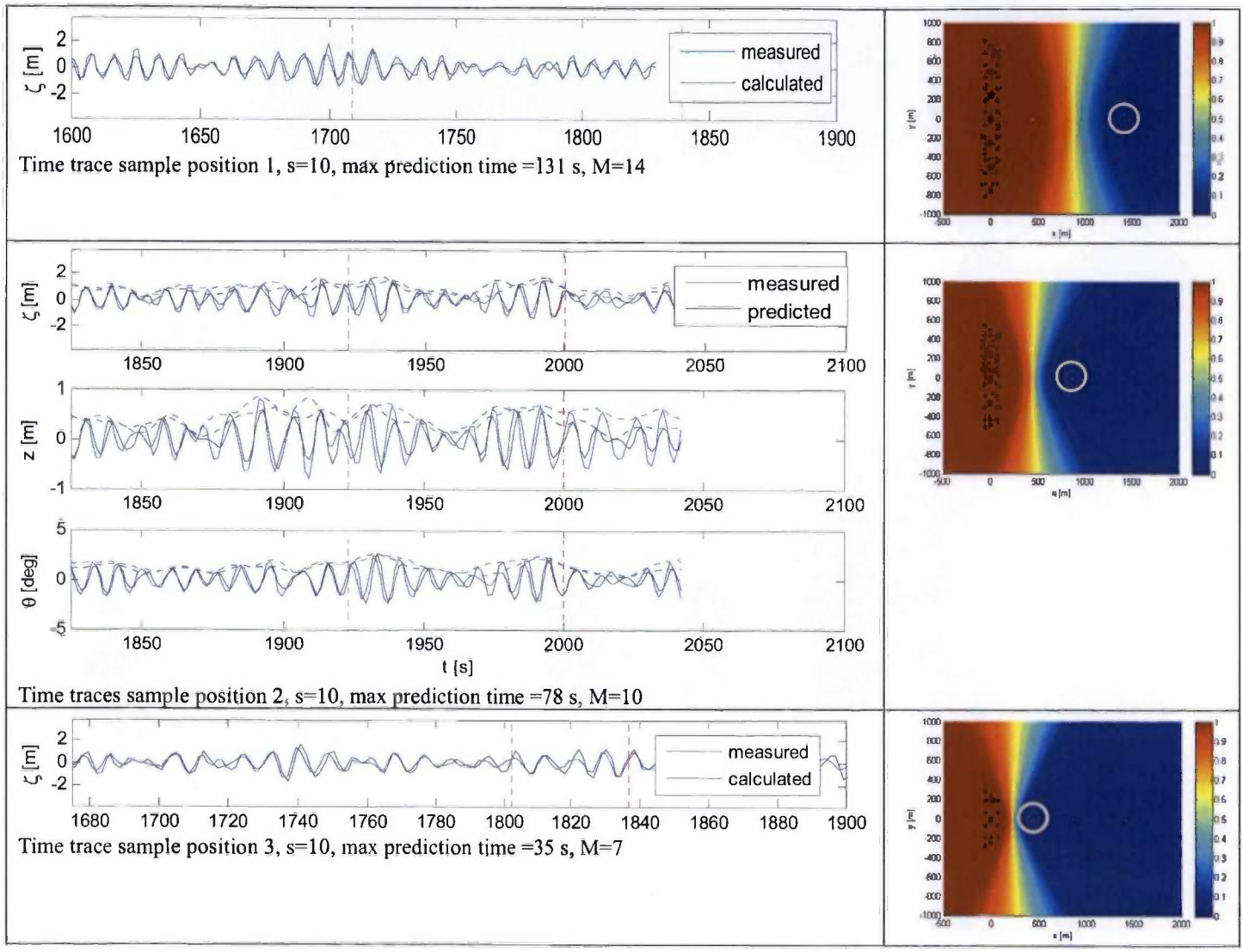

Figure 14, sample time traces for s=10

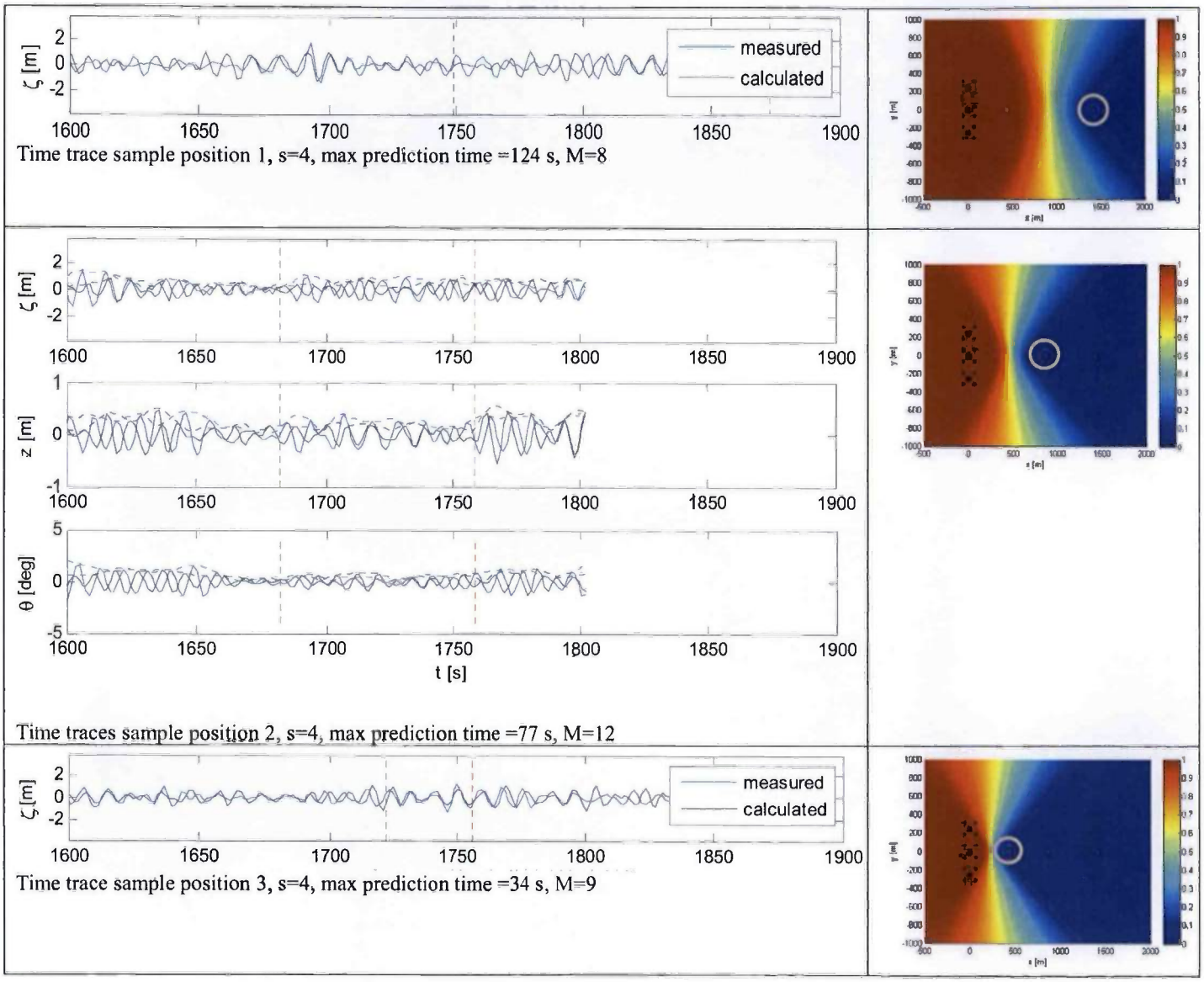

Figure 15, sample time traces for s=4

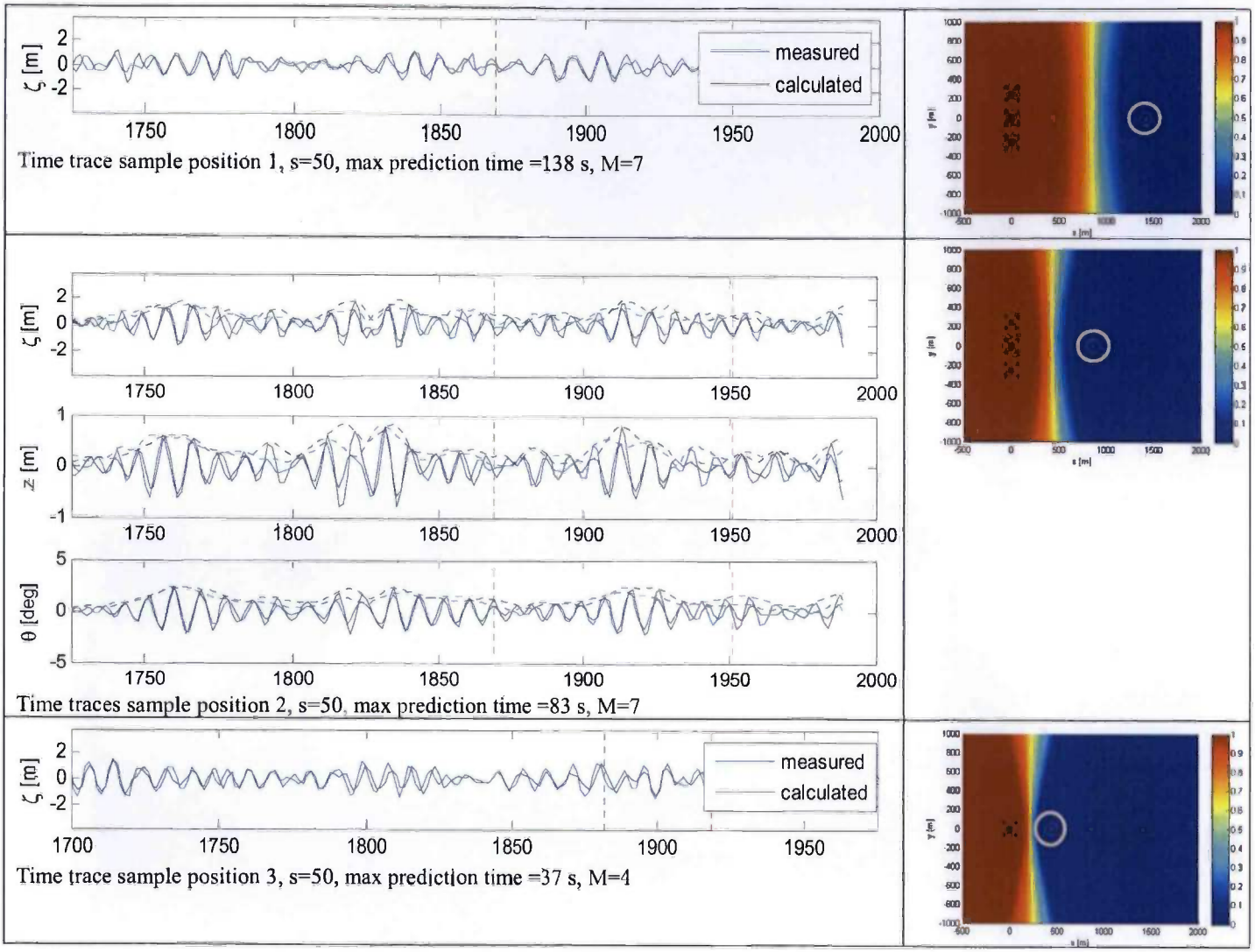

Figure 16, sample time traces for s=50